

## Fluorescent Silk Fibroin Nanoparticles Prepared Using a Reverse Microemulsion

Seung Jun Myung, Hun-Sik Kim, Yeseul Kim, Peng Chen, and Hyoung-Joon Jin\*

Department of Polymer Science and Engineering, Inha University, Incheon 402-751, Korea

Received January 22, 2008; Revised March 25, 2008; Accepted April 3, 2008

**Abstract:** Color dye-doped silk fibroin nanoparticles were successfully fabricated using a microemulsion method. An aqueous silk fibroin solution was prepared by dissolving cocoons (*Bombyx mori*) in a concentrated lithium bromide solution followed by dialysis. A color dye solution was also mixed with the aqueous silk fibroin solution. The surfactants used for the microemulsion were then removed by methanol and ethanol, yielding color dye-doped silk fibroin nanoparticles, approximately 167 nm in diameter. The secondary structure of the nanoparticles showed a  $\beta$ -sheet conformation, as characterized by Fourier transform infrared spectroscopy. The morphology of the nanoparticles was determined by field emission scanning electron microscopy, transmission electron microscopy and atomic force microscopy, and their size and size distribution were measured by dynamic light scattering. The color dye-doped silk fibroin nanoparticles were examined by confocal laser scanning microscopy.

**Keywords:** silk fibroin, nanoparticles, microemulsion.

### Introduction

Nanoparticles, which are colloidal particles whose sizes are below 1  $\mu\text{m}$ , have been extensively studied in various fields of the life sciences such as separation technologies, histological studies, clinical diagnostic assays, drug delivery systems, and cosmetics.<sup>1-3</sup> Their application offers advantages such as easy purification and sterilization, drug targeting possibilities, and sustained release action.<sup>4</sup>

Recently, nanoparticles have been fabricated by various methods, including through the use of microemulsion systems. A microemulsion is a thermodynamically stable dispersion of two immiscible fluids; the system is stabilized by the addition of surfactants. Different types of microemulsions are known, such as water-in-oil (w/o) and oil-in-water (o/w). A w/o microemulsion is formed when water is dispersed in a hydrocarbon based continuous phase. In this case, the thermodynamically driven surfactant self-assembly generates aggregates known as reverse or inverted micelles,<sup>5</sup> of which spherical reverse micelles, whose surface energy is minimized, are the most common form. In particular, microemulsions offer the advantage of a narrow size distribution among the resultant nanoparticles.

For example, poly(lactic-co-glycolic acid) (PLGA) nanoparticles are commonly prepared by emulsion solvent evaporation or by solvent displacement techniques.<sup>6</sup> These nanoparticles are prepared by using a relatively small dis-

persed phase with a medium dispersion ratio and a substantially high stirring speed.<sup>7</sup> Song *et al.* previously reported on the preparation of PLGA nanoparticles by an o/w emulsification/solvent evaporation technique to generate nanoparticles with a size of 150 nm, drug loading of 15.5% (w/w), encapsulation efficiency of 62%, and yield of 85%.<sup>8</sup>

The various conditions under which nanoparticles are produced are influenced by the nature of the process. Dawson and Halbert reported on the fabrication of nanoparticles by an o/w emulsification technique and used the response surface methodology to determine the effects of some variables on the size distribution of PLGA nanoparticles.<sup>9</sup> However, polymer particles are hydrophobic, tend to agglomerate in aqueous media, and swell in organic solvents, resulting in dye leakage.

Silks are naturally produced by spiders or insects such as *Nephila clavipes* and *Bombyx mori*, respectively.<sup>10,11</sup> Silk fibroin is similar to amphiphilic block copolymers, which are repetitive hydrophobic and hydrophilic amino acid sequences.<sup>12</sup> During their processing, fibrous proteins, including silk fibroin in particular, have regular structures due to the assembly by their highly repetitive primary domains.<sup>12-14</sup> The repetitive amino acid sequences of silk fibroin consist of glycine, serine, and alanine. These amino acids play an important role in controlling the assembly of silk fibrous proteins as well as their structures and, ultimately, the properties of the silk fibers.<sup>15</sup> The silk fibroin from *B. mori* is composed of two chains: a heavy chain and a light chain whose molecular weights are approximately 325 kDa and

\*Corresponding Author. E-mail: hjjin@inha.ac.kr

25 kDa, respectively. These chains are linked by a single disulfide bridge. The heavy chain of silk fibroin is composed of crystalline and amorphous domains.<sup>16</sup> Before the silk fibroin is processed, sericin covered with silk fibrils is removed to prohibit the thrombogenic and inflammatory responses of the silk fibroin.<sup>17</sup> The additional properties of silk fibroin include a strong affinity to polysaccharides,<sup>18,19</sup> mechanical properties that include high strength and flexibility<sup>11</sup> and swelling properties that depend on the solution pH.<sup>20</sup> These dynamic properties of the fibroin microstructure make it a good candidate for controlled and sustained drug or gene delivery. Therefore, silk fibroin possessing such amphiphilic, mechanical, and swelling properties is potentially useful for the generation of nanoparticles for encapsulation, molecular imaging, bioassays, and controlled release in drug delivery.<sup>21</sup>

In this work, we studied the preparation of silk fibroin nanoparticles prepared via an w/o microemulsion and investigated the potential of applying these silk fibroin nanoparticles as a biosensor system by encapsulating fluorescent dyes in them.

## Experimental

**Materials.** Cocoons of *B. mori* silkworm silk were supplied by Boeun Traditional Sericulture Farm, Korea. Rhodamine B was purchased from Sigma Aldrich (St. Louis, MO). Commercial Triton X-100 from Daejung Chemicals & Metals Co., Ltd. was used for the preparation of the w/o microemulsion. Reagent grade cyclohexane, methanol, ethanol, and hexanol, all purchased from DC Chemical Co., Ltd, were used without further purification.

**Purification of Silk Fibroin Solution.** Silk fibroin aqueous stock solutions were prepared as previously described.<sup>22</sup> Briefly, cocoons of *B. mori* were boiled for 20 min in an aqueous solution of 0.02 M sodium carbonate, and then rinsed thoroughly with distilled water. After drying, the extracted silk fibroin was dissolved in a 9.3 M LiBr solution at 60 °C for 4 h, yielding a 20% (w/v) solution. This solution was dialyzed against distilled water using Slide-a-Lyzer dialysis cassettes (MWCO 3,500, Pierce) for 3 days to remove the salt. The solution was optically clear after dialysis and was centrifuged to remove the small amounts of silk aggregates that formed during the process; these aggregates are generally from environmental contaminants that are present on the cocoons. The final concentration of the silk fibroin aqueous solution was approximately 8% (w/v). This concentration was determined by weighing the residual solid obtained after drying a known volume of the solution.

**Formation of Silk Fibroin Nanoparticles.** The nanoparticles were prepared using the microemulsion method. The microemulsion solution was prepared by mixing adequate amounts of surfactant, organic solvent, distilled water, and silk aqueous solution. The procedure consisted of mixing

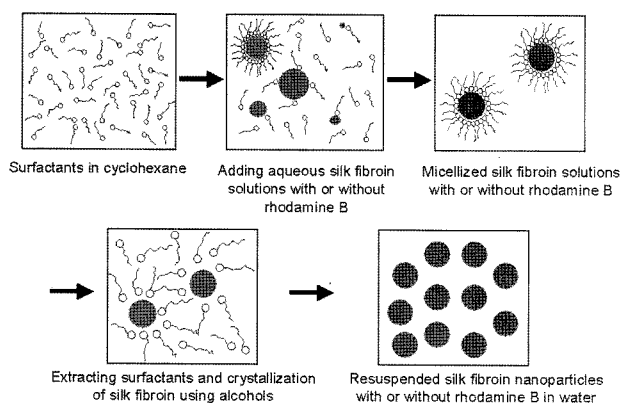
1.77 g of Triton X-100, which is employed as a surfactant, and 7.5 mL of cyclohexane, followed by the addition of 400  $\mu$ L of silk aqueous solution under stirring for 1 min with a vortexer. A mixture of methanol and ethanol was then added to break the microemulsion and recover the particles. The particles were dialyzed successively against ethanol for 24 h and water for 48 h.

**Characterizations.** The surface and morphology of the silk fibroin nanoparticles were observed using field emission scanning electron microscopy (FESEM, S-4300, Hitachi, Japan). The FESEM images were obtained by collecting samples on an aluminum FESEM disk, which was then coated with platinum. The acceleration voltage and working distance for each image were 15 kV and 6 mm, respectively. Transmission electron microscopy (TEM) was performed using a Philips CM 200 unit, operated at an acceleration voltage of 120 kV. The silk fibroin nanoparticles were observed by placing a drop of the sample solution (concentration = 1 mg/mL) onto a 200 mesh copper grid coated with carbon. Approximately 5 min after deposition, the grid was tapped with filter paper to remove the surface water, followed by air-drying. The samples were vacuum-dried for 24 h at room temperature prior to the measurement. Dynamic light scattering (DLS) measurements were performed using a Brookhaven Instruments (Holtville, NY) BI-200SM goniometer and a BI-9000AT digital autocorrelator. All of the measurements were carried out at room temperature. The sample solutions were purified by being passed through a Millipore 0.45  $\mu$ m filter. The scattered light of a vertically polarized He-Ne laser (632.8 nm) was measured at an angle of 90° and collected on an autocorrelator. The hydrodynamic diameters ( $d$ ) of the particles were calculated on the basis of the Stokes-Einstein equation,  $d = kBT/3\pi\eta D$ , where  $kB$  is the Boltzmann constant,  $T$  is the absolute temperature,  $\eta$  is the solvent viscosity, and  $D$  is the diffusion coefficient. The polydispersity factor of the particles, represented as  $\mu_2/\Gamma^2$ , where  $\mu_2$  is the second cumulant of the decay function and  $\Gamma$  is the average characteristic line width, was calculated by the cumulant method.<sup>23</sup> CONTIN algorithms were used in the Laplace inversion of the autocorrelation function to obtain the size distribution. Fourier transform infrared (FT-IR) spectroscopy was performed using a Bruker VERTEX 80v FT-IR spectrometer. A pellet consisting of the nanoparticles mixed with KBr powder was prepared by applying a pressure of 1 ton at room temperature using a Carver laboratory press (Model #3912, Carver Inc., Wabash, IN, USA) and examined with an FT-IR microscope in the transmittance reflection mode. Background measurements were taken with a KBr disk and subtracted from the sample reading. To analyze the fluorescent samples using confocal laser microscopy (MRC-1024, Bio-Rad, UK), the silk fibroin nanoparticles were suspended in distilled water and approximately 20  $\mu$ L of the suspension was put on a glass slide, which was covered with a cover-slip. The

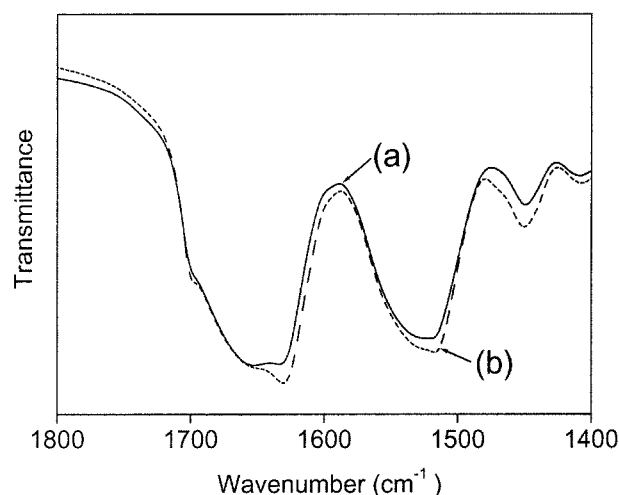
confocal laser microscopy was performed with a 15 mW Krypton/Argon mixed-gas laser (488 nm wavelength). The atomic force microscopy (AFM) measurements were performed using an SPA400 with an SPI 4000 controller, Seiko Instruments, Japan. The cantilever was fabricated from  $\text{Si}_3\text{N}_4$ , and the tip was SI-DF40 (spring constant: 42 N/m; resonance frequency: 250-360 kHz). Ultraviolet-visible (UV-Vis) spectra were obtained with a Hewlett-Packard 8452A spectrophotometer.

## Results and Discussion

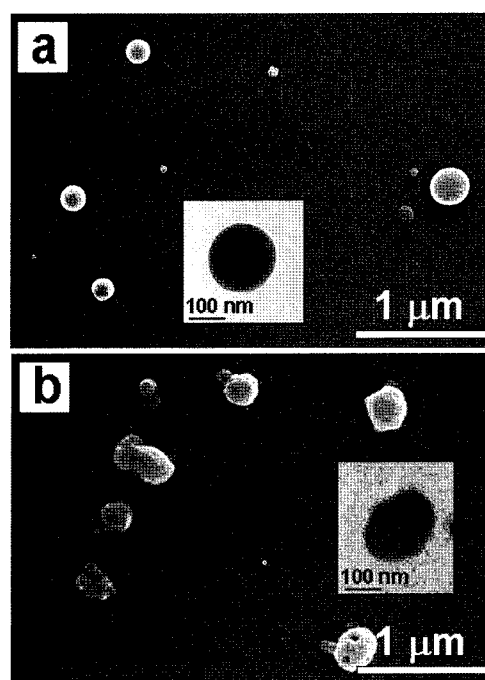
Figure 1 schematically illustrates the preparation method of the fluorescent silk nanoparticles. After methanol and ethanol treatment, the microemulsion templates were removed and the encapsulated silk nanoparticles were concurrently induced to self-assemble to form a crystalline  $\beta$ -sheet structure in order to promote the entrapment of the fluorescent dye (rhodamine B). The  $\beta$ -sheet structure of the silk nanoparticles provides the nanoparticles with stability, due to their insolubility in organic solvents and aqueous media.<sup>24</sup> Methanol has dual functions in this process, the removal of the microemulsions and the dehydration of the silk to induce its assembly into a crystalline form. FT-IR analysis was carried out to study the molecular conformation of silk fibroin nanoparticles. The FT-IR spectra of the silk fibroin nanoparticles with/without fluorescent dye are presented in Figure 2. The absorption was observed at  $1700\text{ cm}^{-1}$  and  $1631\text{ cm}^{-1}$  (amide I), and  $1516\text{ cm}^{-1}$  (amide II), which confirmed that the silk fibroin nanoparticles obtained from regenerated aqueous silk fibroin solution had  $\beta$ -sheet conformation after alcohol treatment.<sup>25</sup> When the fluorescent molecules, i.e., rhodamine B, were encapsulated in the silk fibroin nanoparticles, the peaks corresponding to the  $\beta$ -sheet structure, which were identical with the pure silk nanoparticles, were observed in the spectrum of the fluorescent silk fibroin nanoparticles, indicating that the  $\beta$ -sheet structure was not affected by the fluorescent dye.<sup>26</sup>



**Figure 1.** Scheme of fabrication of silk fibroin nanoparticles with rhodamine B using water-in-oil microemulsion.



**Figure 2.** FT-IR spectra of crystallized silk nanoparticles (a) without and (b) with rhodamine B.



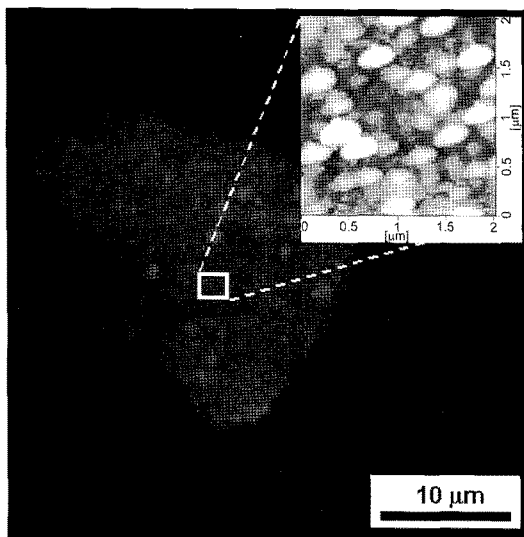
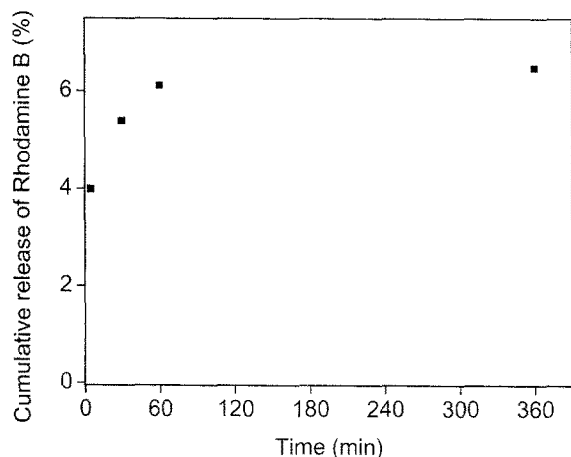
**Figure 3.** FESEM and TEM (inlet) images of (a) silk nanoparticles and (b) silk nanoparticles with rhodamine B.

Figure 3 shows the FESEM and TEM images of the silk nanoparticles with and without rhodamine B. Unlike the finer shape of the silk fibroin nanoparticles without the fluorescent dye, the silk fibroin nanoparticles incorporating the fluorescent dye were rough and spherical. The size of the silk fibroin nanoparticles with/without fluorescent dye was determined by DLS. In both cases, the nanoparticles had an average size of about 167~169 nm (Table I).

The distribution of rhodamine B in the silk fibroin nanoparticles was characterized by confocal laser scanning microscopy (Figure 4). The fluorescent silk fibroin nanopar-

**Table I. Mean Diameter of Silk Nanoparticles in Distilled Water at 25 °C Using DLS**

Sample Name	$d$ (nm)	Polydispersity Factor ( $\mu_2/\Gamma^2$ )
Silk nanoparticles without rhodamine B	167	0.08
Silk nanoparticles with rhodamine B	169	0.13

**Figure 4.** Confocal laser scanning microscopy image of rhodamine B in silk fibroin nanoparticles. Inset image; AFM image of silk nanoparticles with rhodamine B.**Figure 5.** Release of rhodamine B from silk fibroin nanoparticles with time.

ticles exhibited a red color under laser excitation on a confocal microscope. Also, the fluorescent silk fibroin nanoparticles were placed on a silicone wafer and measured by AFM. The AFM image also showed that the fluorescent silk fibroin nanoparticles were spherical and had a uniform size (Figure 4). To demonstrate the stability of the fluorescent silk fibroin nanoparticles, we measured the release profile of rhodamine

B encapsulated in the nanoparticles by UV-Vis spectroscopy (Figure 5). Less than 7% of the rhodamine B was released from the fluorescent silk fibroin nanoparticles into the surrounding media over a period of 360 min. Therefore, the methanol treatment removed the surfactants used as templates and simultaneously induced the formation of  $\beta$ -sheet structures in the silk fibroin nanoparticles.<sup>27</sup> Given that the silk fibroin nanoparticles are nano-scale sized and can be used to encapsulate rhodamine B, they have potentially widespread applicability in molecular imaging and bioassays.

## Conclusions

Fluorescent dye-encapsulated spherical nanoparticles of silk fibroin were simply prepared from an aqueous solution of regenerated silk fibroin by a reverse microemulsion method. The silk fibroin nanoparticles are about 167 nm in diameter and have a spherical shape. The observed stability of the loaded fluorescent molecules in the silk fibroin nanoparticles suggests that they have a strong potential to be used as new and useful devices for molecular imaging and bioassays. Furthermore, owing to the nano-scale size of the silk fibroin particles, their capacity to encapsulate fluorescent dye, and the slow degradation of silk combined with its biocompatibility, silk fibroin nanoparticles are expected to have a significant impact on various biological and medical fields.

**Acknowledgements.** The authors of this paper would like to thank the Korea Science and Engineering Foundation (KOSEF) for sponsoring this research through the SRC/ERC Program of MOST/KOSEF (R11-2005-065).

## References

- (1) C. S. Cho, J. B. Cheon, Y. I. Jeong, I. S. Kim, S. H. Kim, and T. Akaike, *Macromol. Rapid Commun.*, **18**, 361 (1997).
- (2) Y. I. Jeong, J. B. Cheon, S. H. Kim, J. W. Nah, Y. M. Lee, Y. K. Sung, T. Akaike, and C.S. Cho, *J. Control. Release*, **51**, 169 (1998).
- (3) C. S. Cho, Y. I. Jeong, T. Ishihara, R. Takei, J. U. Park, K. H. Park, A. Maruyama, and T. Akaike, *Biomaterials*, **18**, 323 (1997).
- (4) Y. I. Jeong, J. W. Nah, H. C. Lee, S. H. Kim, and C. S. Cho, *Int. J. Pharm.*, **188**, 49 (1999).
- (5) C. Park, M. Rhue, J. Lim, and C. Kim, *Macromol. Res.*, **15**, 39 (2007).
- (6) R. A. Jain, *Biomaterials*, **21**, 2475 (2000).
- (7) R. Arshady, *J. Control. Release*, **17**, 1 (1991).
- (8) C. Song, V. Labhasetwar, L. Guzman, E. Topol, and R. J. Levy, *Proc. Int. Symp. Contr. Rel. Bioact. Mater.*, **22**, 444 (1995).
- (9) G. F. Dawson and G. W. Halbert, *Proc. Int. Symp. Contr. Rel. Bioact. Mater.*, **22**, 424 (1995).
- (10) J. D. van Beek, S. Hess, F. Vollrath, and B. H. Meier, *Proc.*

- Natl. Acad. Sci. U. S. A.*, **99**, 102666 (2002).
- (11) F. Vollrath, B. Madsen, and Z. Shao, *Proc. R. Soc. Lond. B*, **268**, 2339 (2001).
- (12) D. Wilson, R. Valluzzi, and D. Kaplan, *Biophys. J.*, **78**, 2690 (2000).
- (13) D. P. Knight and F. Vollrath, *Philos. Trans. R. Soc. Lond. B*, **357**, 155 (2002).
- (14) F. Vollrath and D. P. Knight, *Nature*, **410**, 541 (2001).
- (15) K. H. Guhrs, K. Weisshart, and F. Grosse, *J. Biotechnol.*, **74**, 121 (2000).
- (16) G. H. Altman, F. Diaz, C. Jakuba, T. Calabro, R. L. Horan, J. Chen, H. Lu, J. Richmond, and D. L. Kaplan, *Biomaterials*, **24**, 401 (2003).
- (17) M. Santin, A. Motta, G. Freddi, and M. Cannas, *J. Biomed. Mater. Res. A*, **46**, 382 (1999).
- (18) L. Rodén, T. Koerner, C. Olson, and N. B. Schwartz, *Fed. Proc.*, **44**, 373 (1985).
- (19) G. Falini, S. Weiner, and L. Addadi, *Calcified Tissue Int.*, **72**, 159 (2003).
- (20) J.-H. Yeo, K.-G. Lee, Y.-W. Lee, and S. Y. Kim, *Eur. Polym. J.*, **39**, 1195 (2003).
- (21) H.-J. Jin and D. L. Kaplan, *Nature*, **424**, 1057 (2003).
- (22) S. Sofia, M. B. McCarthy, G. Gronowicz, and D. L. Kaplan, *J. Biomed. Mater. Res.*, **54**, 139 (2001).
- (23) Y. Song, C. Park, and C. Kim, *Macromol. Res.*, **14**, 235 (2006).
- (24) S. Hofmann, C. T. Wong Po Foo, F. Rossetti, M. Textor, G. Vunjak-Novakovic, D. L. Kaplan, H. P. Merkle, and L. Meinel, *J. Control. Release*, **111**, 219 (2006).
- (25) K. Kesenci, A. Motta, L. Fambri, and C. Migliaresi, *J. Biometer. Sci.-Polym. E*, **12**, 337 (2001).
- (26) H.-J. Jin, J. Park, V. Karageorgiou, U.-J. Kim, R. Valluzzi, P. Cebe, and D. L. Kaplan, *Adv. Func. Mat.*, **15**, 1241 (2005).
- (27) B. Zumreoglu-Karan, H. Mazi, and A. Guner, *J. Appl. Polym. Sci.*, **83**, 2168 (2002).